Article

Not peer-reviewed version

An Inulin-Type Fructan CP-A from Codonopsis pilosula Alleviated 5-Fluorouracil-Induced Intestinal Mucositis via ERK/MLCK/MLC2 Pathway and Regulation of Gut Microbiota

Jiangtao Zhou , Deyun Li , Jiajing Wang , Zhuoyang Cheng , Changjian Wang , Xuepeng Zhang , Xiexin Xu , Jianping Gao *

Posted Date: 26 December 2023

doi: 10.20944/preprints202312.1959.v1

Keywords: inulin-type fructan CP-A; intestinal mucositis; inflammation; ERK/MLCK/MLC2 signaling pathway; mucosal barrier; intestinal microbiota

Article

An Inulin-Type Fructan CP-A from *Codonopsis pilosula* Alleviated 5-Fluorouracil-Induced Intestinal Mucositis via ERK/MLCK/MLC2 Pathway and Regulation of Gut Microbiota

Jiangtao Zhou [1,2,3,†], Deyun Li [1,†], Jiajing Wang [1], Zhuoyang Cheng [1,2,3], Changjian Wang [1], Xuepeng Zhang [1], Xiexin Xu [1] and Jianping Gao [1,2,3,*]

[1] School of Pharmacy, Shanxi Medical University, Taiyuan 030001, China
[2] Medicinal Basic Research Innovation Center of Chronic Kidney Disease, Ministry of Education, Shanxi Medical University, Taiyuan 030001, China
[3] Shanxi Provincial Key Laboratory of Drug Synthesis and Novel Pharmaceutical Preparation Technology, Shanxi Medical University, Taiyuan 030001, China
* Correspondence: jpgao123@163.com
† These authors contributed equally to this work

Abstract: Intestinal mucositis (IM) is a common adverse effect of chemotherapy, limiting its clinical application. Edible Chinese medicine, specifically *Codonopsis pilosula*-derived CP-A, with anti-inflammatory and gastrointestinal protective effects. The present work was to investigate CP-A's role in ameliorating IM and its mechanism using *in vitro* and rat models. Western blot, immunohistochemical (IHC) and real-time PCR (RT-PCR) analyses were used to assess protein expression related to the extracellular-regulated protein kinases (ERK)/myosin light chain kinase (MLCK)/myosin light chain 2 (MLC2) signaling pathway and tight junction proteins. Enzyme-linked immunosorbent assay (ELISA) was conducted to measure inflammatory factors, and 16S rRNA Amplicon Sequencing was employed for cecum content analysis. The results indicated that CP-A could restore body weight, food intake and histopathological changes in IM rats. Besides, abnormal MLCK activation induced by 5-fluorouracil (5-FU) was attenuated by CP-A via the ERK/MLCK/MLC2 pathway. CP-A treatment improved tight junction protein levels and reduced inflammatory factor expression. On the other hand, intestinal flora experiment demonstrated that CP-A intervention could increase the abundance of *lactobacillus*. In conclusion, CP-A mitigates 5-FU-induced IM by inhibiting the ERK/MLCK/MLC2 pathway, reducing the expression of inflammatory factors, improving the intestinal mucosal barrier and regulating intestinal flora. This study sheds light on CP-A's therapeutic potential in IM treatment, providing insights for future research.

Keywords: Inulin-type fructan CP-A; Intestinal mucositis; Inflammation; ERK/MLCK/MLC2 signaling pathway; Mucosal barrier; Intestinal microbiota

1. Introduction

Many cancers, including stomach, esophageal, breast and head cancer, rely on 5-FU treatment [1, 2]. 5-FU is the first-line treatment for colorectal cancer [3, 4]. However, the use of 5-FU can result in severe adverse reactions, such as IM [5]. The clinical manifestations of IM include diarrhea, nausea and vomiting, which cause intense discomfort to patients and seriously limit the use of chemotherapeutic drugs [6, 7]. Unfortunately, there are currently no effective medications for alleviating the pain associated with intestinal mucositis, therefore, it is necessary to identify and develop treatments that can effectively alleviate the symptoms and enhance the quality of life for patients undergoing chemotherapy. 5-FU exhibits cytotoxic effects on intestinal epithelial cells, resulting in damage to the intestinal mucosal barrier and the release of pro-inflammatory factors [8]. Tight junction proteins are

 doi:10.20944/preprints202312.1959.v1

essential components of the intestinal barrier 9. The primary mode through which 5-FU reaches the intestinal mucosal barrier is by degrading the tight junction proteins 10. In addition, 5-FU disrupts the intestinal flora 11, 12. These factors offer potential avenues for addressing IM.

Proinflammatory factors play an important role in the occurrence and development of inflammation 13, 14. Overexpression of tumor necrosis factor-alpha (TNF-α) and interferon gamma (IFN-γ) is often detected in cases of IM 15, 16. ERK and MLCK play central roles in the protection of intestinal epithelial tight junction 17. By promoting the phosphorylation of MLC2, MLCK is activated by Phospho-ERK1/2, leading to the destruction of intestinal tight junction and degradation of tight junction proteins such as Claudin-1, Occludin, F-actin and Zonula occludens-1 (ZO-1) 18, 19. TNF-α activation of ERK1/2 promotes ERK phosphorylation, thus activating the ERK/MLCK/MLC2 pathway 19. In addition, the overexpression of IFN-γ is involved in the activation of MLCK which up-regulate the expression of Claudin-2 and promote interleukin (IL)-13 release 20. Once the intestinal barrier is breached, an increase in intestinal epithelium permeability permits endotoxins and macromolecules to enter the cells freely, causing the release of IL-6, IL-8, TNF-α and IFN-γ, which will aggravate inflammatory response 18. Moreover, the destruction of the intestinal mucosal barrier is accompanied by disturbances in the intestinal flora 9, 21. Therefore, the inhibition of TNF-α and IFN-γ overexpression and the regulation of ERK/MLCK/MLC2 pathway protect the intestinal mucosal barrier and reduce inflammation. A stable and healthy microbiome is essential for the proper functioning of the gut 8. Many studies have indicated that chemotherapy-induced gastrointestinal diseases are often accompanied by disturbance of intestinal flora 10. Dysregulation of intestinal flora leads to disruption of intestinal homeostasis and intestinal mucus barrier integrity 9, 11. There is increasing evidence that 5-FU-induced IM can cause the imbalance of intestinal flora, the abundance of harmful bacteria increases and the abundance of probiotics decreases 10, 12. Thus, regulating intestinal flora and increasing the abundance of probiotics may be a potential treatment for 5-FU-induced IM.

Traditional Chinese Medicine (TCM) and natural products extracted from TCM have a long history of clinical application in the treatment of various diseases, including IM 22. *Codonopsis pilosula*, an edible herbal medicine widely used for improving poor gastrointestinal function in traditional Chinese medicine, is derived from the roots of *Codonopsis pilosula* (Franch.) Nanf., *Codonopsis pilosula* (Franch.) Nannf. var. *modesta* (Nannf.) L.T. Shen and *Codonopsis tangshen* Oliv. In recent days, the edible plant has been listed by National Health Commission of China as a substance that is both food and traditional Chinese medicine. Over the past years, *Codonopsis pilosula*, the plant homologous to food and medicine is known for its anti-ulcerative colitis effects, its role in regulating intestinal flora, and its ability to decrease inflammatory factor levels 23, 24. The main active constituents of *Codonopsis pilosula* are polysaccharides, lignans and polyacetylenes 25. Additionally, the anti-inflammatory effects of polysaccharides from *Codonopsis pilosula* have been reported 24, 26. CP-A is an inulin-type fructan and represents the most active ingredient in *Codonopsis pilosulae* polysaccharides. Nevertheless, research on IM treatment is rare. Meanwhile, it's *in vivo* and *in vitro* anti-IM mechanisms remain unclear. Hence, this study selected IEC-6 cells and Sprague-Dawley (SD) rats as experimental subjects to investigate the mechanism of CP-A treatment for 5-FU-induced chemotherapeutic enteritis. This study will provide valuable insights for the development of improved treatments for IM, addressing a critical need in clinical oncology.

2. Materials and Methods.

2.1. Chemicals and Reagents

CP-A (Figure 1a, MW: 3.6kDa), an inulin-type fructan, was isolated from *Codonopsis pilosula* as previously described 27. 5-FU (F6173) was purchased from Macklin Biochemical Co., Ltd. (Shanghai, China). Bifid. Triple Viable Capsules Dissolving at Intestines (BTC) were purchased from Jincheng HEALTH Pharmaceutical Co., Ltd. (Jincheng, Shanxi, China). Primary antibodies against rat MLC2 (DF7911 1:2000), Phospho-MLC2 (Ser15 AF8618 1:1000) were purchased from Affinity Biosciences Co., Ltd. (OH, United States). MLCK (21642-1-AP 1:1000), ERK1/2 (11257-1-AP 1:5000), Phospho-

Preprints (www.preprints.org) | NOT PEER-REVIEWED | Posted: 26 December 2023 doi:10.20944/preprints202312.1959.v1

ERK1/2 (Thr202/Tyr204 28733-1-AP 1:2000), Beta Actin (20536-1-AP, 1:2000), Claudin-2 (26912-1-AP, 1:1000), Occludin (27260-1-AP, 1:5000), ZO-1 (21773-1-AP, 1:5000) were purchased from Proteintech Group, Inc. (Wuhan, China). Claudin-1 (bs-1428R, 1:1000) and F-actin (bs-1571R) were obtained from Beijing Biosynthesis Biotechnology Co. Ltd. (Beijing, China). The secondary antibodies were obtained from ImmunoWay Biotechnology (TX, United States). All ELISA kits were acquired from Jiangsu Meimian Industrial Co., Ltd. (Jiangsu, China). All the other materials were of analytical grade.

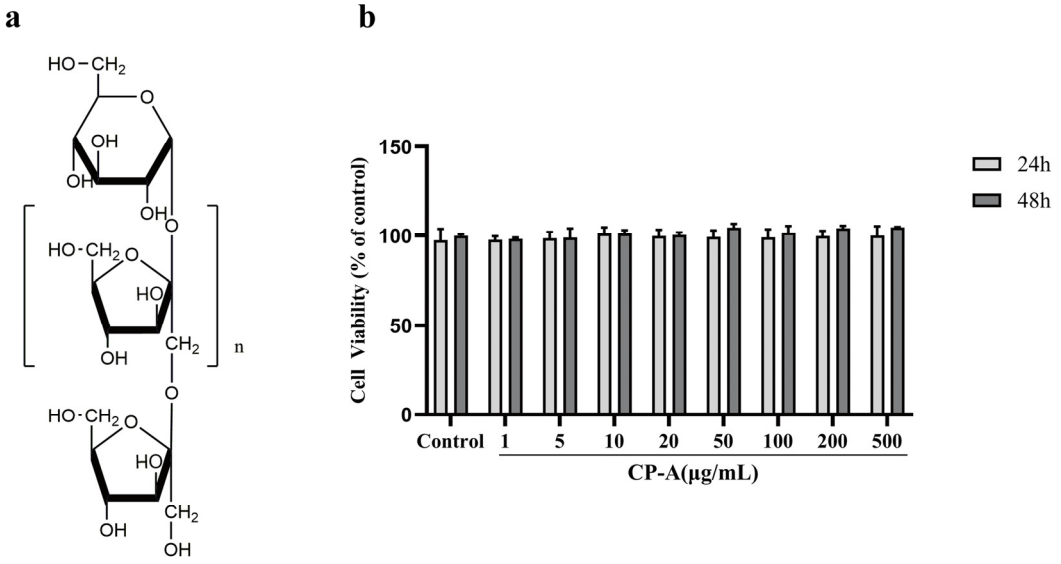

Figure 1. Cytotoxicity of CP-A to IEC-6 cells (**a**) The chemical structure of CP-A (**b**) Cell viability was measured by MTT. Values were represented as mean±SEM (n = 3).

2.2. Cells Culture and MTT Assay

The rat intestinal epithelial cell line IEC-6 was acquired from the BeNa Culture Collection (BNCC100548) and maintained in complete high-glucose DMEM culture medium (Thermo Fisher Gibco, MA, USA, Cat. No. C11995500BT) with 10% fetal bovine serum (FBS, AusGeneX, Australia, Cat. No. 10100147) and 1% streptomycin/penicillin (Gibco, NY, USA, Cat. No. 15240-062) at 37°C in 95% air and 5% CO_2. Cell viability was assessed using the 3-(4,5-dimethylthiazol-2-yl)-2,5-diphenyltetrazolium bromide (MTT) assay after treatment with different concentrations of CP-A (0, 1, 5, 10, 20, 50, 100, 200 and 500 μg/mL) for 24 h. Briefly, IEC-6 cells (2.0×10^3 cells/well) in the logarithmic (log) growth phase were inoculated into 96-well plates (100 μL/well) and made to adhere for 24 h. Thereafter, the medium was substituted with CP-A and treated for 24 h. Then, the different concentrations of CP-A were substituted with MTT (100 μL) to each well at a final concentration of 5 mg/mL and incubated for 4 h. Subsequently, removing the medium and Dimethyl sulfoxide (DMSO, 100 μL) was added to each well. After shaking the plates for 10 min, cell viability was evaluated at 570 nm. The MTT assay was repeated three times to ensure data reproducibility.

2.3. Total RNA Extraction and Quantitative Real-Time PCR

IEC-6 cells were seeded in 6-well plates (2.0×10^5 cells/well) and cultured for 24 h to adhere. Cells were treated with different concentrations of CP-A for 1 h and then incubated with or without 5-FU (10 μg/mL) for 24 h 28. Total RNA was extracted from IEC-6 cells using *TransZol Up* reagent (Transgen, Beijing, China, Cat. No. ET111-01). RNA concentration was detected using an Eppendorf Bioluminometer D30 (Roche, Mannheim, Germany). Subsequently, a cDNA Synthesis Supermix kit (Transgen, Beijing, China, Cat. No. AT311-02) was used to reverse transcribe total RNA into cDNA according to the manufacturer's instructions. Finally, Tip Green qPCR Supermix (Transgen, Beijing,

 doi:10.20944/preprints202312.1959.v1

China, Cat. No. AQ141-01) was used to conduct RT-PCR analysis on a Light Cycler[96] Real-Time PCR System (Roche, Mannheim, Germany). The experiment was conducted according to the reaction program (one cycle of 94 °C for 30 s, followed by 40 cycles of 94 °C for 5 s and 60 °C for 30 s). The primer sequences for the target genes, such as MLCK, ERK1/2, TNF-α, IL-4, IL-6 and IL-10 used in this study are shown in Table S1 (see Supplementary material 1). The relative quantification of all mRNA expression was performed using the $2^{-\Delta\Delta Ct}$ method. GAPDH was purchased from Sangon Biotech (Shanghai, China, Cat. No. B661204-0001) as an internal reference for the normalization of the target genes.

2.4. Experimental Animals

Male SD rats [SPF grade, weighing 200±20 g, approval number: SCXK (Jing) 2019-0010] were provided by Beijing Sipeifu Biotechnology Co., Ltd. All animals used in this study were fed with 12 h light/dark cycle and allowed free access to food and clean water under a regulated condition of room temperature (20-24 °C) and relatively constant humidity. All experimental protocols were approved by the Animal Experimental Ethics Committee of the Shanxi Medical University. In accordance with the regulations on human care and use of laboratory animals, all reasonable measures were taken to minimize animal suffering.

2.5. Establishment of 5-FU-Induced Intestinal Mucositis

All rats were allowed to acclimate for a week and then randomly divided into six groups (n=12): control group, 5-FU group (50 mg/kg, intraperitoneal injection, *i.p.*), BTC group (250 mg/kg, intragastric administration, *i.g.*) and CP-A groups (15, 30, 60 mg/kg, *i.g.*). In the control group, rats were intraperitoneally injected with 0.8 mL 0.9% saline solution per 200g of body weight, while the other group rats were administered 5-FU over the first three days. The vehicle, BTC, or different doses of CP-A were orally administered to all rats daily during the experiment (Figure 2a). Rats were deeply anesthetized with 10% chloral hydrate 24 h after the final treatment. Blood samples were obtained from the abdominal aorta for biochemical analysis, and the cecal contents were collected to analyze the intestinal flora. Small-intestinal tissues were rapidly harvested and rinsed with cold PBS. Ileum samples of all rats (0.5 × 0.5 cm) were fixed in 4% paraformaldehyde and embedded in paraffin for subsequent experiments, while other intestinal tissues were stored at -80 °C for biochemical analysis.

2.6. Histopathological Evaluation

Paraffin blocks containing tissue sections of 5-μm-thickness were cut and stained with hematoxylin and eosin (H&E) to evaluate ileum tissue damage using an Olympus light microscope (Tokyo, Japan).

2.7. Immunohistochemical Staining

IEC-6 cells were inoculated into clean microscope cover glass placed in 6-well plates (2.0×10^5 cells/well), followed by treatment as before. The glass plates containing the cells were removed for immunohistochemical analysis.

Paraffin sections and slides of the cells were dewaxed. After blocking endogenous peroxidase activity, sections were incubated overnight at 4 °C with ZO-1, Occludin, Claudin-1, F-actin, MLCK and Phospho-MLC2 antibodies, followed by the addition of secondary anti-rabbit antibodies. This was followed by one-hour incubation indoors. DAB staining was performed after 40 min, followed by restraint using hematoxylin. Images were captured using a Nikon Eclipse Ci scanning microscope (Nikon Instruments, Melville, NY).

Preprints (www.preprints.org) | NOT PEER-REVIEWED | Posted: 26 December 2023 doi:10.20944/preprints202312.1959.v1

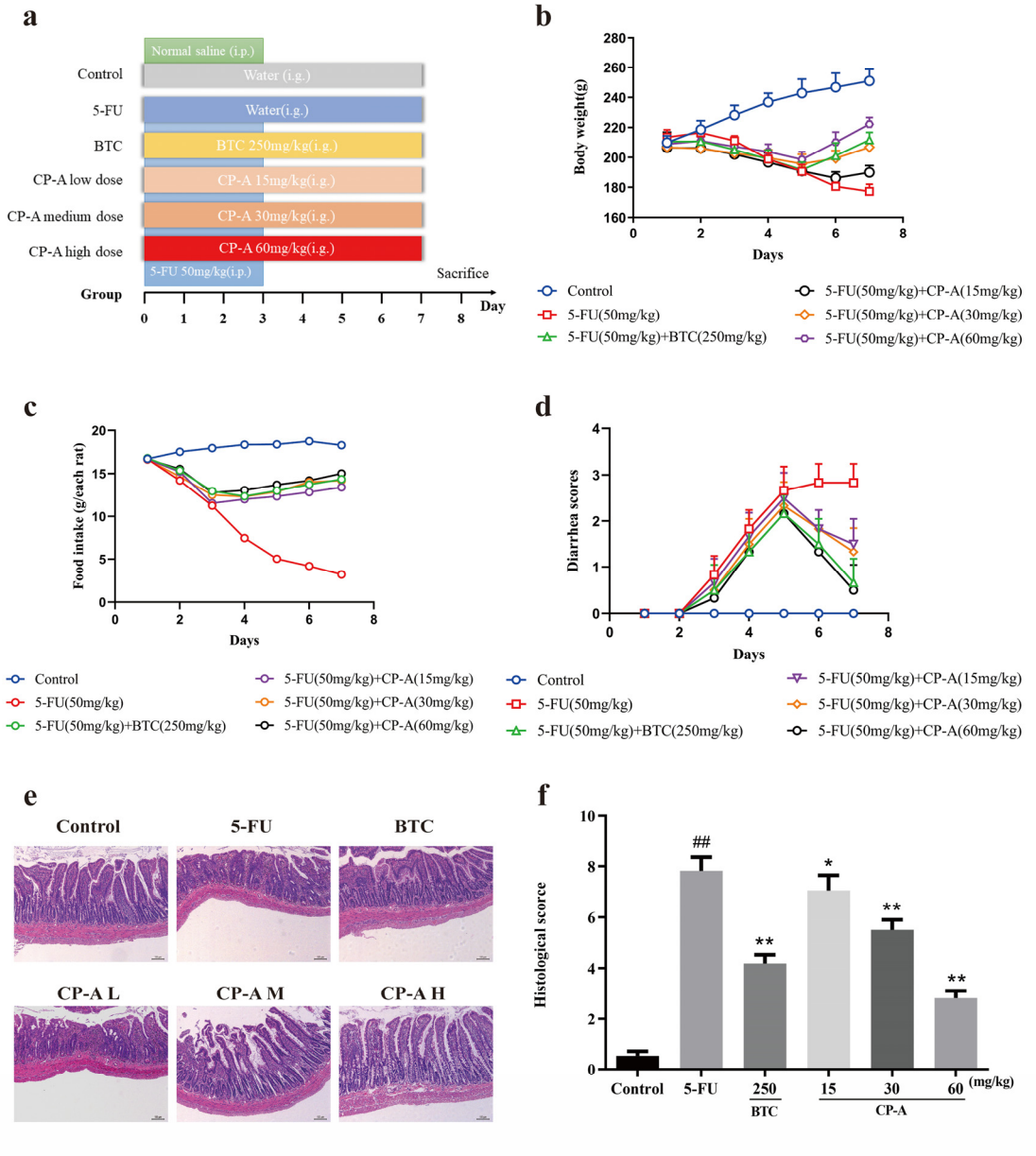

Figure 2. CP-A alleviates the macroscopic manifestation of intestinal mucositis in rats. (**a**) Experimental design and study grouping. (**b**) Body weight changes (n = 6) (**c**) Food intake (n = 6). (**d**) Diarrhea scores (n = 6). (**e**) H&E-stained sections from ileums (n = 3, magnification 50×). (**f**) Histopathological scores. CP-A L, low dose of CP-A (15 mg/kg, *i.g.*); CP-A M, medium dose of CP-A (30 mg/kg, *i.g.*); CP-A H, high dose of CP-A (60 mg/kg, *i.g*). Values were represented as mean±SEM. $^{\#}p < 0.05$ and $^{\#\#}p < 0.01$ versus control group, $^{*}p < 0.05$ and $^{**}p < 0.01$ versus 5-FU group.

2.8. ELISA Analysis

Fresh blood samples were centrifuged to collect serum (1000 rpm for 10 min at 4 °C), which the IEC-6 cells seeded onto six-well plates as previously described. The cell supernatant was collected for analysis. Serum and IEC-6 supernatant levels of TNF-α, IL-4, IL-6, IL-8, IL-10, IL-13 and IFN-γ were measured using ELISA according to the manufacturer's instructions.

2.9. Western Blotting Experiments

Total protein from cell samples or small intestine tissues was extracted using RIPA Lysis buffer (containing 10 μL 100× PMSF, 10 μL phosphatase inhibitor per 1mL) via ultrasonic crusher (Scientz, Zhejiang, China) and the tissue grinder (Servicebio, Wuhan, China). The BCA Protein Assay Kit

 doi:10.20944/preprints202312.1959.v1

(Keygen Biotech, Jiangsu, China, Cat. No. KGP902) was used to quantify the protein concentration. Equal amounts of protein were separated using electrophoresis on sodium dodecyl sulfate-polyacrylamide gels (SDS-PAGE) and transferred onto polyvinylidene difluoride (PVDF) membranes. The membranes were then blocked with a rapid blocking buffer for 15 min before being incubated overnight at 4°C with various antibodies, including MLC2, Phospho-MLC2, MLCK, ERK1/2, Phospho-ERK1/2, ZO-1, Occludin, Claudin-1, Claudin-2 and β-actin. Finally, the membranes were incubated with secondary antibodies for 1 h. The membranes were washed three times with TBST solution for 5 min each time, followed by incubation with primary and secondary antibodies. The Bio-Rad ChemiDoc XRS imaging system was used to detect protein band intensity after the addition of Electro-Chemi-Luminescence (ECL) reagent (Seven Beijing, China). The analysis was conducted using Image Lab Software version 6.0 (Bio-Rad Laboratories).

2.10. Gut Microbiota Analysis

Sequencing was performed by Shanghai Personal Biotechnology Co., Ltd. (Shanghai, China). Briefly, total genomic DNA was isolated from the cecal contents using the OMEGA Soil DNA Kit (M5635-02) (Omega Bio-Tek, Norcross, GA, USA), according to the manufacturer's instructions. The V3–V4 regions of the 16S rRNA were amplified using forward primer 338F (5'-ACTCCTACGGGAGGCAGCA-3') and reverse primer 806R (5'-GGACTACHVGGGTWTCTAAT-3'). The DADA2 plug-in was used for quality filtering, denoising, merging and chimera removal. QIIME2 and R packages (v3.2.0) were utilized for processing sequence data, while ASV-level alpha diversity indices such as Chao1 Shannon Simpson were calculated via ASV table analysis. Beta diversity analysis [Bray-Curtis metrics via principal coordinate analysis (PCoA)] showed the structural variation of microbial communities in each sample group, while LDA Effect Size (LEfSe) detected differentially abundant taxa across groups using default parameters.

2.11. Data Analysis

All study outcomes were presented as the Mean ± Standard error of mean (SEM) from three independent experiments. Statistical analyses were performed using SPSS software (version 26.0; IBM, New York, NY, USA) and GraphPad Prism software (version 8.0; San Diego, USA). Student's t-test was used to compare two groups, while one-way analysis of variance (ANOVA) was employed for multiple comparisons of three or more groups, with *p*-values ($p < 0.05$) considered statistically significant.

3. Reaults

3.1. Cytotoxic Effects of CP-A on IEC-6 Cells

IEC-6 cells were treated with varying concentrations of CP-A for either 24 or 48 h, and no significant cytotoxicity was observed based on the MTT assay results, as shown in Figure 1b. Low and high doses of CP-A at 100 μg/mL and 200 μg/mL, respectively, were selected for subsequent *in vitro* studies.

3.2. Protective Effects of CP-A on 5-FU-Induced Intestinal Mucositis in Rats

The study established a rat model involving continuous intraperitoneal injection of 5-FU for 3 days, starting from the first day. The experimental design is displayed in Figure 2a. Apart from the control group, rats in the other groups experienced weight loss from the second day. Following BTC or CP-A administration, this trend was reversed. Rats in the BTC, CP-A medium and high-dose groups gradually gained weight from the fifth day, and the rats in the CP-A low-dose group gradually gained weight from the sixth day. The rats in the control group continued to gain weight during the experiment, while those in the 5-FU group rats continued to lose weight at the second day (Figure 2b). Food intake and diarrhea showed similar changes (Figure 2c and 2d). Histopathological results revealed varying degrees of damaged intestinal epithelium caused by 5-FU. The rats in the 5-

Preprints (www.preprints.org) | NOT PEER-REVIEWED | Posted: 26 December 2023 doi:10.20944/preprints202312.1959.v1

FU group had the most severe intestinal damage, with significant mucosal necrosis compared to the control group. Administration of BTC and CP-A resulted in a dose-dependent alleviation of intestinal damage, as depicted in Figure 2e, while the histopathological scores showed a notable reduction compared to the group administered with only 5-FU ($p < 0.01$), as presented in Figure 2f.

3.3. Effect of CP-A on Inflammatory Cytokines

Assays conducted on IEC-6 cells revealed that following the administration of 5-FU, there was an up-regulation of expression levels of TNF-α, IFN-γ, IL-6, IL-8, and IL-13. Conversely, levels of IL-4 and IL-10 were significantly reduced. However, the intervention by BTC and CP-A reversed this trend, especially at a concentration level of CP-A (200 μg/mL and 60 mg/kg) ($p < 0.01$) (Figure 3).

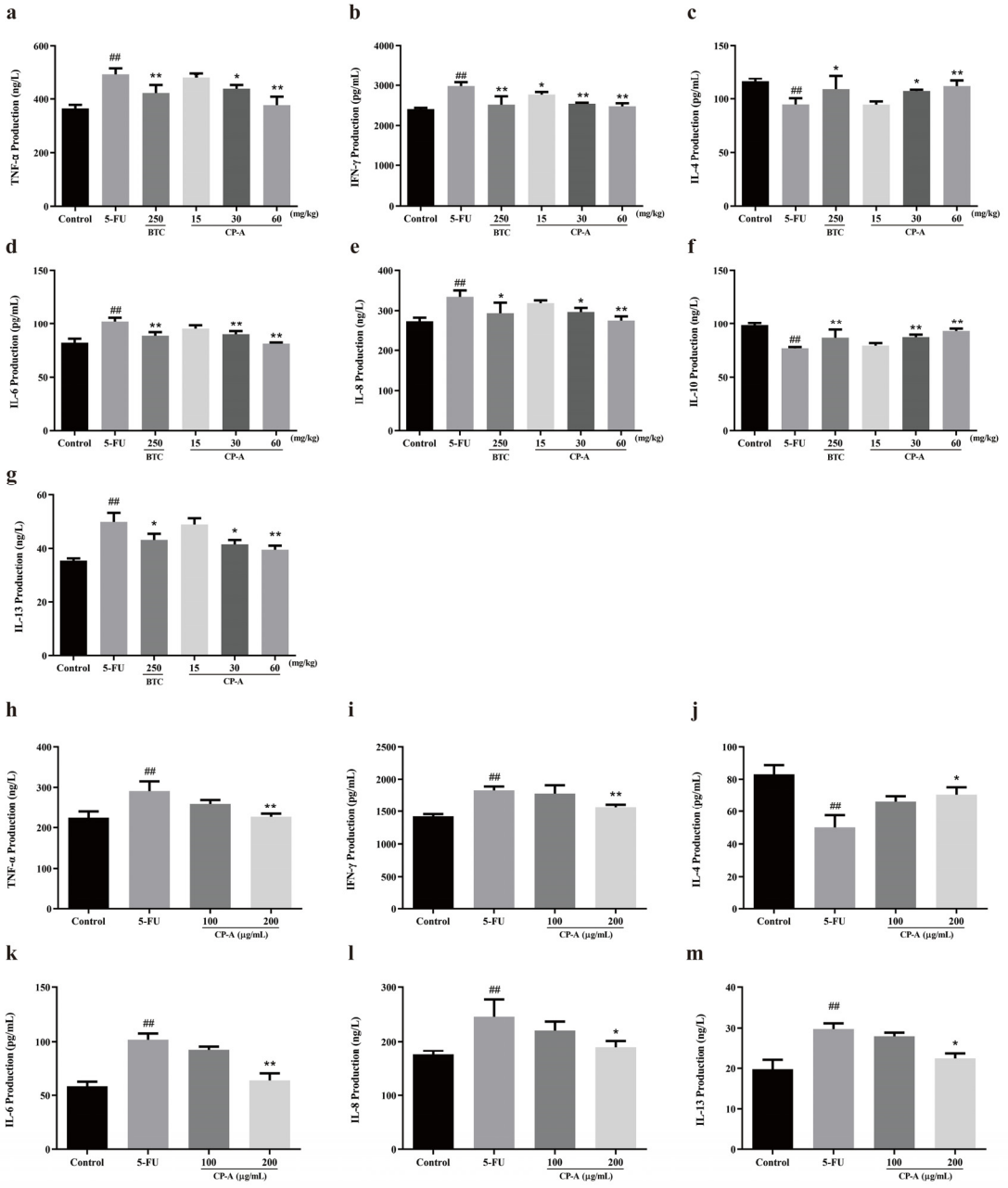

Figure 3. Effects of CP-A on inflammatory cytokines in 5-FU induced rats and IEC-6 cells. (**a-g**) The levels of TNF-α, IFN-γ, IL-4, IL-6, IL-8, IL-10 and IL-13 in rat serum (n = 6). (**h-m**) The levels of TNF-α, IFN-γ, IL-4, IL-6, IL-8 and IL-13 in cellular supernatant (n = 6). Values were represented as mean±SEM. $^{\#}p < 0.05$ and $^{\#\#}p < 0.01$ versus control group, $^{*}p < 0.05$ and $^{**}p < 0.01$ versus 5-FU group.

Preprints (www.preprints.org) | NOT PEER-REVIEWED | Posted: 26 December 2023 doi:10.20944/preprints202312.1959.v1

3.4. Effect of CP-A on ERK/MLCK/MLC2 Signaling Pathway

After demonstrating that CP-A improved inflammatory cytokines levels, western blot analysis revealed a change in ERK/MLCK/MLC2 pathway following CP-A administration. We detected various proteins (ERK1/2, p-ERK1/2, MLCK, MLC2 and p-MLC2) associated with ERK/MLCK/MLC2 pathway in both IEC-6 cells and small intestinal tissues. As shown in Figure 4a-d and 4f-i, p-ERK1/2 was activated in the 5-FU group, and this activation was diminished after CP-A administration ($p < 0.01$). MLCK which is downstream of p-ERK1/2, was significantly downregulated compared to the group administered only 5-FU ($p < 0.01$). Western blot results obtained from rats treated with 5-FU and IEC-6 cells treated with 5-FU were similar. Protein immunohistochemical staining also yielded results consistent with those of the western blot analysis, as depicted in Figure 4e and 4j.

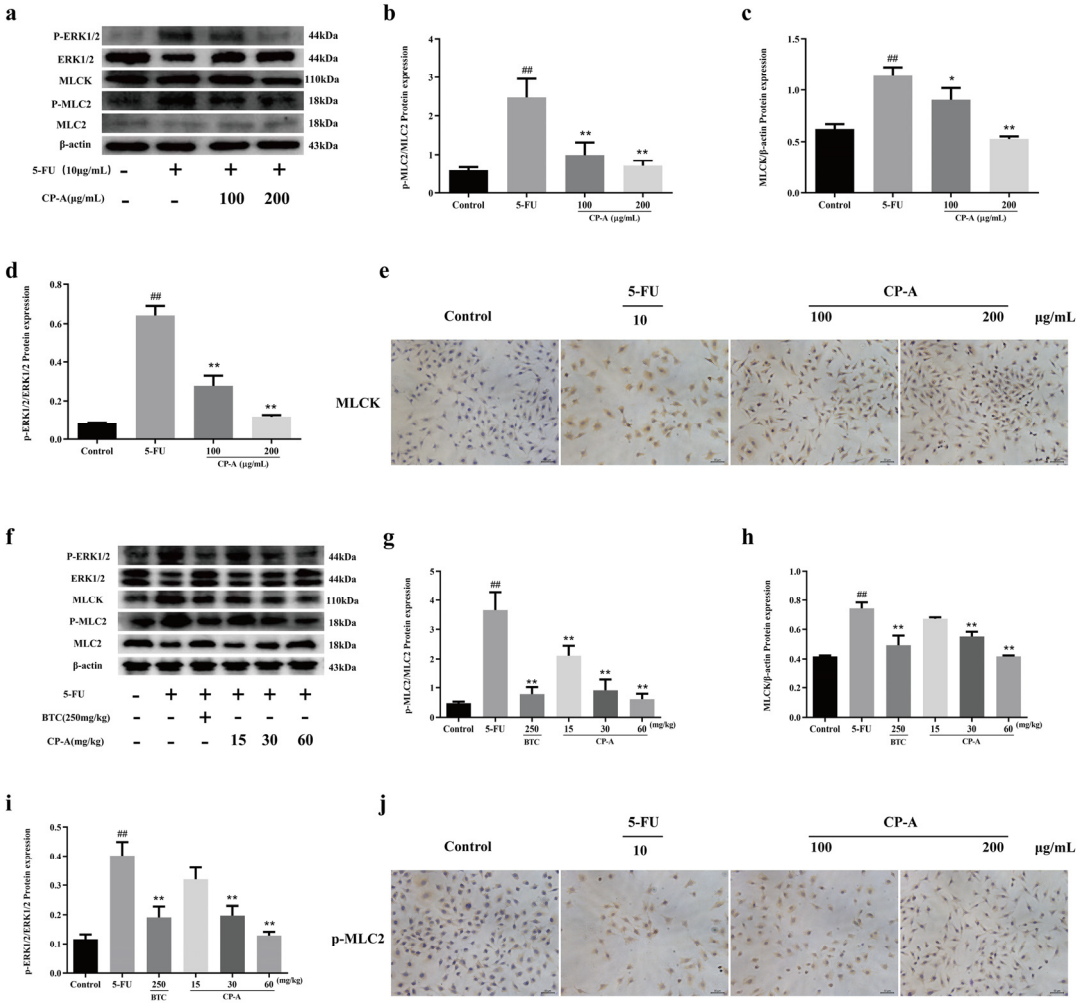

Figure 4. Effects of CP-A on ERK/MLCK/MLC2 signaling pathway proteins in 5-FU induced rats and IEC-6 cells. (**a-d**) Expression of MLC2, p-MLC2, MLCK, ERK1/2 and p-ERK1/2 in IEC-6 cells. (**e**) MLCK protein in IEC-6 cells (magnification 100×). (**f-i**) Expression of MLC2, p-MLC2, MLCK, ERK1/2 and p-ERK1/2 in intestinal. (**j**) p-MLC2 protein in IEC-6 cells (magnification 100x). Values were represented as mean±SEM (n = 3). $^{\#}p < 0.05$ and $^{\#\#}p < 0.01$ versus control group, $^{*}p < 0.05$ and $^{**}p < 0.01$ versus 5-FU group.

3.5. Effect of CP-A on Intestinal Mucosal Barrier Proteins

Western blotting was performed to determine the expression of tight junction proteins in IEC-6 cells and immunohistochemical staining to detect the expression of the proteins in the small intestine tissues. The results proved that 5-FU significantly downregulated the expression of Occludin, ZO-1

 doi:10.20944/preprints202312.1959.v1

and Claudin-1 and upregulated the expression of Claudin-2. Nevertheless, these effects were reversed by CP-A. Similarly, 5-FU remarkably reduced the concentrations of Occludin, ZO-1, Claudin-1 and F-actin compared to the control group. After CP-A and BTC administration, the concentrations of these tight junction proteins increased (Figure 5a-f). The above data manifested that CP-A plays an important role in the treatment of cellular and intestinal tissue barrier dysfunction.

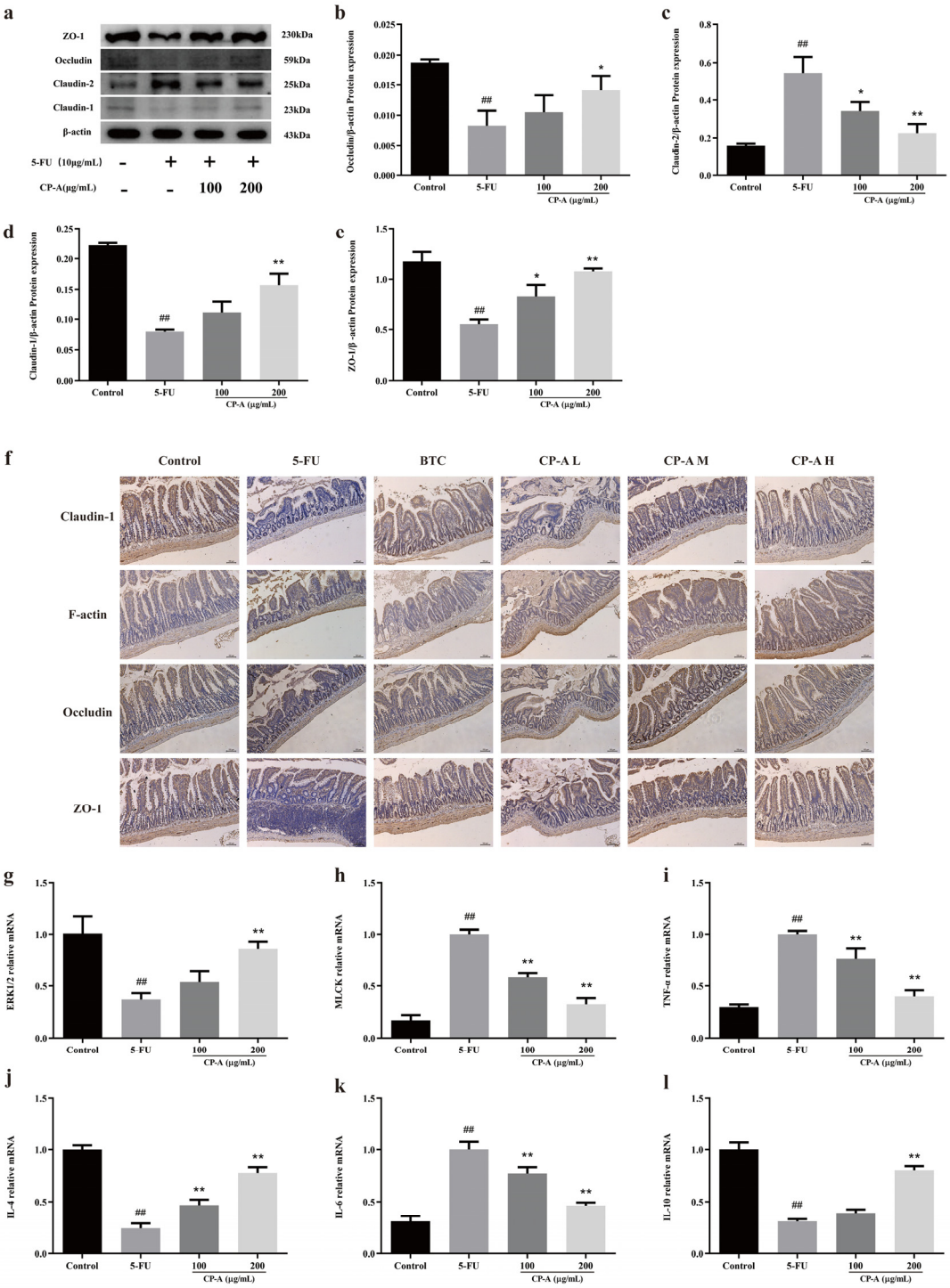

Figure 5. Effects of CP-A on intestinal mucosal barrier proteins. (**a-e**) Expression of Claudin-1, Claudin-2, Occludin and ZO-1 proteins in IEC-6 cells. (**f**) Expression of Claudin-1, F-actin, Occludin and ZO-1 proteins in intestinal (magnification 50x). (**g-l**) Relative mRNA expression of ERK1/2, MLCK, TNF-α, IL-4, IL-6 and IL-10. Values were represented as mean±SEM (n = 3). $^{\#}p < 0.05$ and $^{\#\#}p < 0.01$ versus control group, $^{*}p < 0.05$ and $^{**}p < 0.01$ versus 5-FU group.

Preprints (www.preprints.org) | NOT PEER-REVIEWED | Posted: 26 December 2023 doi:10.20944/preprints202312.1959.v1

Then, RT-PCR was used to assess the mRNA levels of MLCK, ERK1/2, TNF-α, IL-4, IL-6 and IL-10. In the 5-FU group, there was a significant increase in the expression of MLCK, TNF-α and IL-6 compared to the control group. However, the expression of ERK1/2, IL-4 and IL-10 showed the opposite pattern. The RT-PCR results were similar to those of ELISA, western blotting and immunohistochemical staining (Figure 5g-l).

3.6. Effect of CP-A on Microbial Diversity

The rarefaction curve of the Shannon index reflects the detection depth of microorganisms in the sample (Figure 6a). The Venn diagram shows the number of ASVs/OTUs common and unique to each group (Figure 6b). Overlap analysis showed that 549 ASV/OTUs were present in all six groups. In addition, 8996, 9081, 8513, 7989, 8431 and 6856 unique ASVs/OTUs were observed in the control, 5-FU, BTC and CP-A (L, M, and H) groups, respectively. To evaluate the richness and diversity of the microbiota community, we utilized the Chao 1, Shannon and Simpson indices for alpha diversity analysis (Figure 6c). The rats in the 5-FU group had the highest Chao 1, Shannon and Simpson indices. After CP-A treatment, these indices decreased. These results suggested that 5-FU increased the diversity of the microbial community. Beta diversity was used to measure the similarity of microbial communities in each group. PCoA based on the Bray-Curtis distance showed the largest differences between the control, 5-FU and high-dose CP-A groups (Figure 6d). This result indicates that CP-A treatment might affect community structure.

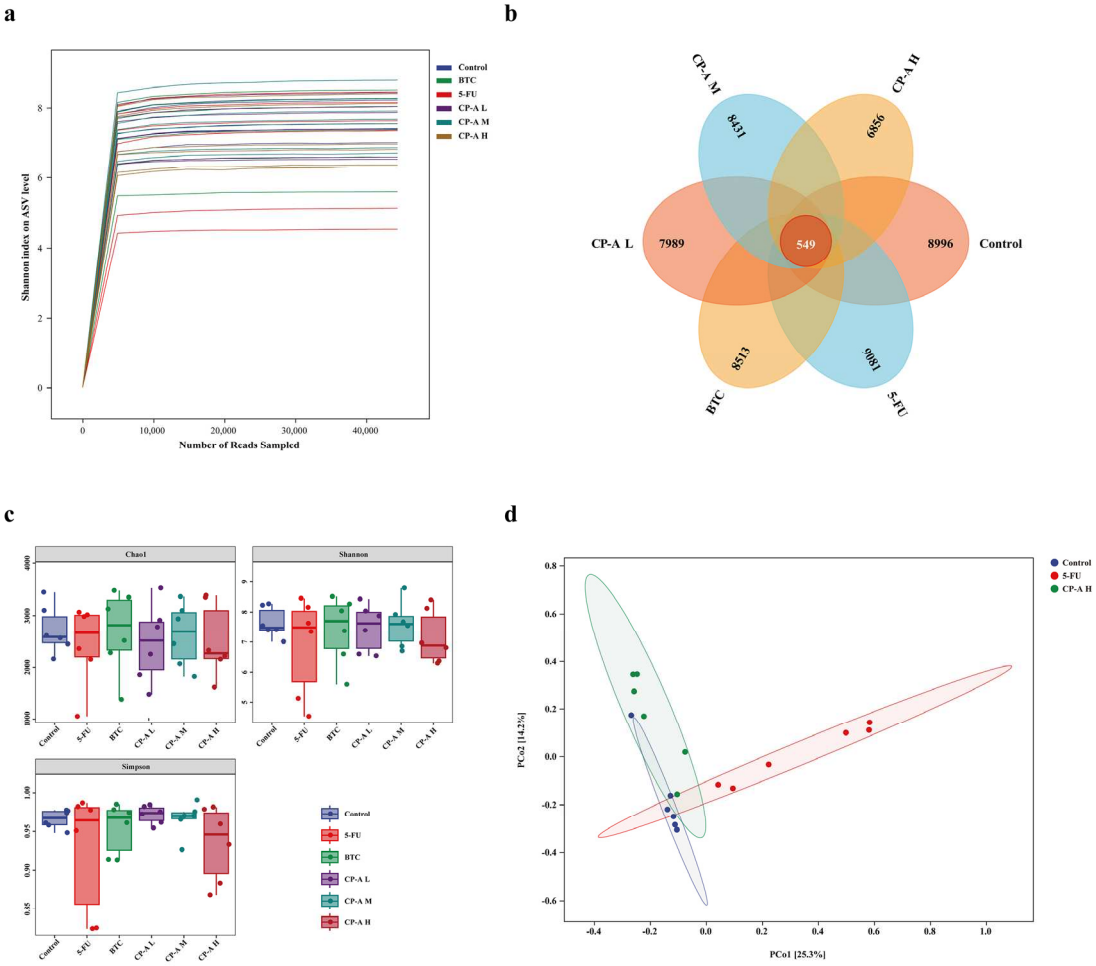

Figure 6. Effects of CP-A on ASV and microbial diversity analysis. **(a)** rarefaction curve of Shannon index. **(b)** Venn diagram of ASVs. **(c)** Alpha diversity (Chao1 index, Shannon index, Simpson index); **(d)** Beta diversity (bray-curtis). Values were represented as mean±SEM (n = 6).

 doi:10.20944/preprints202312.1959.v1

3.7. Taxonomic Composition Analysis of Microbial Community

The gut microbial composition was determined at the Phylum, Class, Order, *Family*, and *Genus* levels. At the Phylum level, *Firmicutes*, *Proteobacteria*, *Bacteroidetes*, and *Actinobacteria* were the most abundant, and their abundance were more than 95% (Figure 7a and Table S2). After 5-FU injection, the abundance of *Firmicutes* and *Bacteroidetes* decreased from 89.49% to 62.86% and from 6.97% to 6.54%, respectively. In addition, the abundances of *Proteobacteria* and *Actinobacteria* increased to 27.03% and 2.57% by 5-FU. After CP-A intervention, their abundance recovered to normal levels.

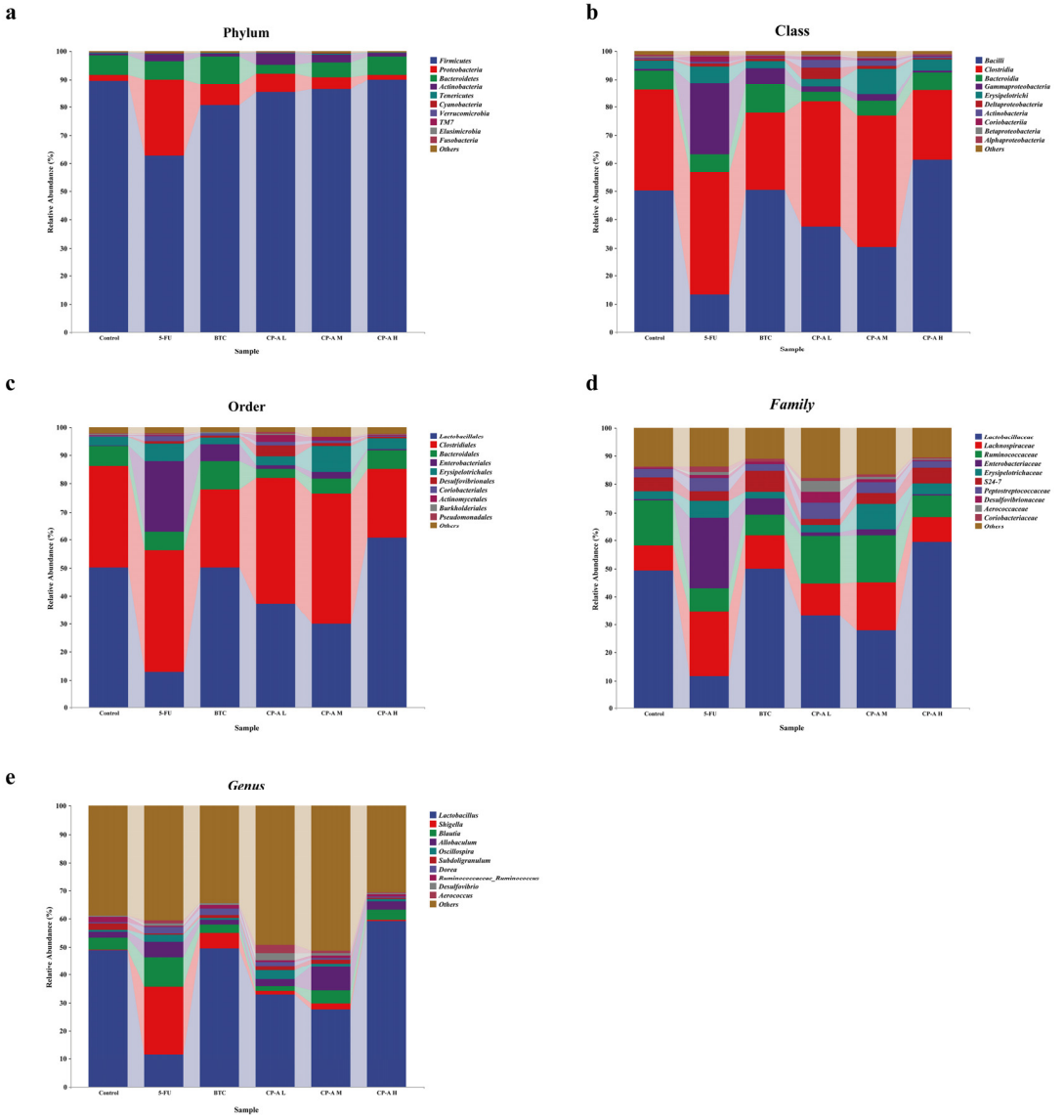

Figure 7. Taxonomy analysis of microbiota community at Phylum, Class, Order, *Family* and *Genus* levels (n = 6).

We calculated the flora abundance at the class level, and the results are shown in Figure 7b and Table S3. *Bacilli*, *Clostridia*, *Bacteroidia* and *Erysipelotrichi* were the most abundant in the control group, but the abundance of *Gammaproteobacteria* was the second highest in the 5-FU group ($p < 0.01$ vs. control and CP-A H). After 5-FU administration, the abundance of *Bacilli* decreased notably ($p < 0.01$), whereas that of *Clostridia* increased to 43.28%, making it the highest in the 5-FU group. At the Order level, *Lactobacillales*, *Clostridiales*, *Bacteroidales* and *Erysipelotrichales* were the most abundant in control rats, whereas *Clostridiales* and *Enterobacteriales* were the two most abundant in 5-FU rats (Figure 7c and Table S4). Furthermore, the abundance of *Enterobacteriales* increased markedly in the 5-FU group ($p < 0.01$ vs. control and CP-A H). *Lactobacillaceae* were the dominant bacteria in the control group,

Preprints (www.preprints.org) | NOT PEER-REVIEWED | Posted: 26 December 2023 doi:10.20944/preprints202312.1959.v1

and *Enterobacteriaceae* were the dominant bacteria in the 5-FU group at the *Family* level (Figure 7d and Table S5). After CP-A and BTC treatment, *Enterobacteriaceae* was observably decreased ($p < 0.05$). *Lactobacillus* was the characteristic bacteria in the control group, and *Shigella* was the characteristic bacteria in the 5-FU group at the *genus* level. *Lactobacillus* decreased notably in the 5-FU group compared to that in the control group ($p < 0.01$). After CP-A and BTC treatment, *Lactobacillus* was observably increased ($p < 0.01$) (Figure 7e and Table S6).

3.8. Effect of CP-A on Intestinal Mucosal Barrier Proteins

LEfSe analysis was used to identify biomarkers in each group (Figure 8a and 8b). *g_Prevotella*, *g_Streptococcus*, *g_Acetobacter* and *g_Ralstonia* were marker bacterial genera in the control group, whereas *g_Olsenella* and *g_Bacteroides* were highly expressed in the 5-FU group. After BTC and CP-A administration, *g_Caulobacter* was the main bacterium in the BTC group, while *g_Lactobacillus* and *g_Veillonella* were the marker bacteria in the CP-A H group.

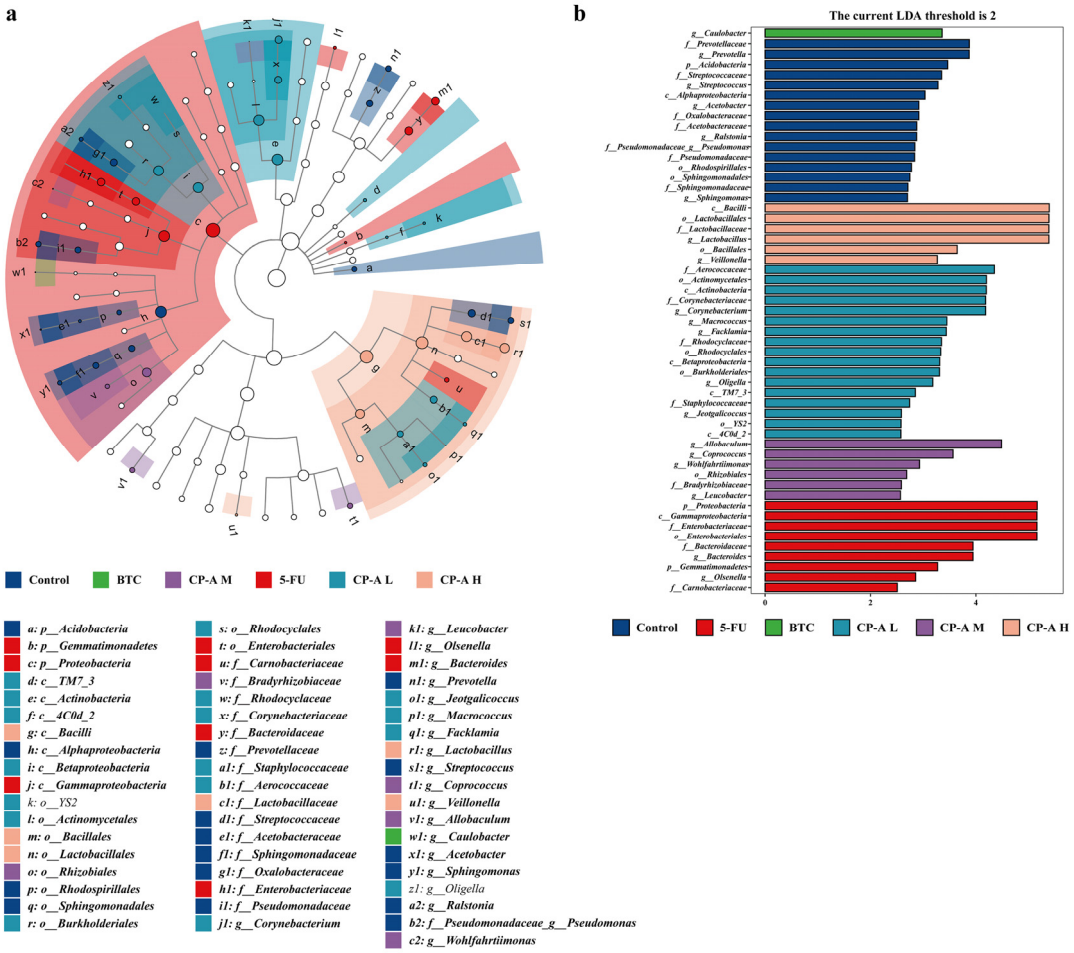

Figure 8. LEfSe analysis (n = 6) **(a)** Each group of LEfSe analysis by cladogram. **(b)** LDA distribution histogram of significantly different species in each group.

4. Discussion

The main manifestations of IM induced by 5-FU were diarrhea and decreased food intake 29. This is primarily attributed to the damage inflicted upon the integrity of the intestinal mucosa by 5-FU 30. Previous research has indicated that the mucosa lining of the small intestine is particularly susceptible to the detrimental effects of 5-FU treatment 31, 32. Our study aimed to investigate the effect of CP-A on inflammation induced by 5-FU, both *in vitro* and *in vivo*. Our findings demonstrated

that CP-A effectively restored body weight and food intake, alleviated diarrhea symptoms and reduced intestinal mucosal damage in rats with 5-FU-induced IM. These results suggest that CP-A has an inhibitory effect on 5-FU-induced IM and probably plays a role in inhibiting the ERK/MLCK/MLC2 signaling pathway and regulating microbial structure.

Inflammation can occur due to the release of pro-inflammatory factors and often accompanies various immune responses and processes 33, 34. TNF-α, an inflammatory cytokine, is produced by macrophages and monocytes during inflammation, and it is involved in the conduction of various intracellular signals, leading to cell necrosis or apoptosis 35. TNF-α is also an essential pro-inflammatory cytokine detectable in various inflammatory conditions 36, 37. Endotoxins and exotoxins are the most common inducers of cytokine production 38. As inflammation progresses, the generation of inflammatory cytokines including, TNF-α and IFN-γ, orchestrates the innate immune response against infections 39. However, excessive expression of TNF-α and IFN-γ is harmful, and IL-6 and IL-8 also contribute to inflammation 40. Furthermore, both IL-4 and IL-10 were found to downregulate MCP-1 production, which plays a crucial role in intestinal inflammation, not only in Caco2 cells but also in freshly isolated epithelial cells 41. Our *in vitro* and *in vivo* experiments revealed that CP-A exhibited remarkable anti-inflammatory effects by modulating inflammatory cytokine levels in IEC-6 cells stimulated with 5-FU and in rats with intestinal mucositis. CP-A significantly reduced the levels of IL-6, IL-8, TNF-α and IFN-γ, while enhancing IL-4 and IL-10 expression in both cell cultures and the rat model rat.

Tight-junction proteins play a protective role in the intestinal mucosal barrier, and their degradation is often observed during intestinal inflammation 9. An increasing number of studies have shown that the degradation of tight junction proteins is accompanied by the activation of ERK and MLCK 17, 20. MLCK promotes the phosphorylation of MLC2, which increases the expression of p-MLC2 and produces ATP, which degrades tight junction proteins 36. Moreover, a 5-FU-induced increase in TNF-α and IFN-γ expression not only promotes the occurrence of inflammation but also acts as an activator of ERK and MLCK 9. Furthermore, the activation of MLCK leads to increased secretion of IL-13 and Claudin-2 expression20, 42. The ERK/MLCK/MLC2 signaling pathway becomes activated due to elevated p-ERK1/2 levels and MLC2 phosphorylation following 5-FU administration in both cellular and rat models. However, treatment with CP-A significantly reduced p-ERK1/2 levels, along with MLC2 phosphorylation and MLCK expression, thereby deactivating the ERK/MLCK/MLC2 signaling pathway. Thus, the expression of Claudin-1, F-actin, Occludin, and ZO-1 in the cells and small intestine was upregulated, whereas the expression of Claudin-2 and IL-13 were downregulated.

To assess the potential cytotoxicity of CP-A on IEC-6 cells, we performed an MTT assay, which indicated that CP-A promotes cell growth without causing cytotoxic effects. Another study also supported CP-A's lack of cytotoxicity 43. Western blot and IHC results revealed that CP-A significantly restores Claudin-1, Occludin and ZO-1 levels while down-regulating IL-6, IL-8, TNF-α and IFN-γ.

Additionally, the gut microbiota plays a crucial role in maintaining intestinal homeostasis as it acts as an ecological barrier44. Imbalances within the gut microbiota can lead to various adverse effects, such as diarrhea and indigestion, associated with inflammatory bowel diseases, such as ulcerative colitis or Crohn's disease 4, 45. Interestingly, our sequencing data revealed that 5-FU disrupted the overall structure and abundance of the gut microbiota and altered the relative abundance of specific bacterial genera known to inhabit the intestine 11, 12, 21. The results of α-diversity analysis indicated that high-dose CP-A decreased the richness and diversity of the flora. However, the results of β-diversity analysis indicated that the high-dose CP-A group and the control group had similar microflora structures, whereas the 5-FU group displayed a significantly distinct microflora structure. Hence, CP-A effectively stabilized the microbial community.

Firmicutes, *Proteobacteria*, *Bacteroidetes* and *Actinobacteria* are the four dominant bacteria in normal organisms, with *Firmicutes* having the highest relative abundance. Our findings are consistent with those of previous studies showing that 5-FU can alter the gut microbiota composition by decreasing *Firmicutes* abundance while increasing *Proteobacteria* prevalence. This shift in composition may affect

dietary energy absorption, given *Firmicutes*'s role in this process 46. Research has shown that dysregulation of the gut flora accompanies 5-FU-induced intestinal mucositis, leading to increased Proteobacteria abundance and gastrointestinal disorders such as enteritis and diarrhea 4. Interestingly, CP-A reversed these changes in the abundance of Firmicutes and Proteobacteria, offering a potential avenue for mitigation.

To further investigate bacterial genera specifically altered by 5-FU and CP-A treatment, we examined their relative abundances among the rats used in this study. 5-FU significantly increased the relative abundance of *Shigella* and decreased the relative abundance of *Lactobacillus*; however, CP-A restored the relative abundance of these genera. Notably, high-dose CP-A treatment resulted in a significant increase in the relative abundance of *Lactobacillus* compared to that in the other groups. *Lactobacillus* is an intestinal probiotic that effectively combats acute diarrhea and intestinal mucosal lesions 47. *Shigella* is a small gram-negative bacterium that invades the intestinal epithelium and causes shigellosis, also known as bacillary dysentery. The main cause of bacterial diarrhea is *Shigella* infection, which is highly lethal in malnourished people 48. Therefore, CP-A administration was found to alleviate 5-FU-induced intestinal mucositis in rats by reducing the prevalence of *Shigella* and increasing the prevalence of *Lactobacillus*.

5. Conclusion

These results suggested that CP-A may exert its beneficial effects by decreasing inflammatory factors, improving intestinal mucosal barrier damage and modulating the gut microbiota. Specifically, CP-A was able to inhibit MLCK expression, suppress TNF-α and IFN-γ signaling pathways, and prevent degradation of Claudin-1, F-actin, Occludin and ZO-1 proteins while also reducing Claudin-2 and IL-13 expression levels. CP-A reduces pro-inflammatory cytokine levels (IL-6, IL-8, TNF-α and IFN-γ), increases anti-inflammatory cytokine levels (IL-4 and IL-10), stabilizes microbial structure, and balances microbial communities by up-regulating *Lactobacillus* relative abundance while down-regulating *Shigella* relative abundance. In conclusion, our work provided potential novel strategy for treatment of chemotherapy-induced IM by *Codonopsis pilosula*. Moreover, it also provided experimental evidence for the application of in patients with IM caused by chemotherapy. Nevertheless, as this study was only performed the molecular mechanism and changes in the gut microbiota in rats unilaterally, which may have limitations. In our future endeavor, more in-depth investigations on the anti-IM effect of CP-A, including genetically defective animals or fecal bacteria transplantation would be performed. These future studies should be conducted to gain further insight into the mechanism of action and highlight the potential of CP-A as a promising candidate drug.

Supplementary Materials: The following supporting information can be downloaded at the website of this paper posted on Preprints.org. Supplementary Material 1: Table S1 Sequences of the primers used in the RT-PCR. Table S2 Relative abundance of the most representative phyla in experimental rats. Table S3 Relative abundance of the most representative classes in experimental rats. Table S4 Relative abundance of the most representative orders in experimental rats. Table S5 Relative abundance of the most representative families in experimental rats. Table S6 Relative abundance of the most representative families in experimental rats. Supplementary Material 2: Original gels used in Figure 4 and Figure 5.

Author Contributions: Jiangtao Zhou: Conceptualisation, Methodology, Investigation, Writing – original draft, Writing-review & editing, Funding acquisition. Deyun Li: Conceptualisation, Investigation, Resources, Writing – original draft, Writing- review & editing, Data curation. Jiajing Wang: Data curation, Formal Analysis, Resources, Investigation. Zhuoyang Cheng, Changjian Wang, Xuepeng Zhang, Xiexin Xu: Investigation, Resources. Jianping Gao: Conceptualization, Methodology, Writing-original draft, Writing-review & editing, Funding acquisition.

Funding: This work was supported by National Natural Science Foundation of China (81904031), National Key Research and Development Program of China (2019YFC1710800), Natural Science Foundation of Shanxi Province (201901D211325) and Science Research Start-up Fund for Doctor of Shanxi Medical University (XD1802).

Institutional Review Board Statement: The animal experimental scheme strictly followed the ethical code of Animal Care and Use Committee of Shanxi Medical University and the Guidelines for The Care and Use of Laboratory Animal (approval number: SYXK (Jing) 2017-0005).

 doi:10.20944/preprints202312.1959.v1

Data Availability Statement: The cecum microbiota gene sequence dataset presented in this study has been made available at the NCBI online repository: NCBI; Submission ID: SUB14100411; BioProject ID: PRJNA1054780.

Conflicts of Interest: The authors declare that they have no known competing financial interests or personal relationships that could have appeared to influence the work reported in this paper.

Abbreviations

IM Intestinal mucositis
5-FU 5-fluorouracil
IHC Immunohistochemical
RT-PCR Real-time PCR
ERK Extracellular-regulated protein kinases
MLCK Myosin light chain kinase
MLC2 Myosin light chain 2
ELISA Enzyme-linked immunosorbent assay
TNF-αTumor necrosis factor-alpha
IFN-γ Interferon gamma
ZO-1 Zonula occludens-1
IL Interleukin
BTC Bifid. Triple Viable Capsules Dissolving at Intestines
MTT 3-(4,5-dimethylthiazol-2-yl)-2,5-diphenyltetrazolium bromide
DMSO Dimethyl sulfoxide
PBS Phosphate-buffered saline
H&E Hematoxylin and eosin
PCoA Principal coordinate analysis
LEfSe LDA Effect Size
FBS Fetal bovine serum
BSA Bovine serum albumin
SPF Specific pathogen-free
SD Sprague–Dawley
TCM Traditional Chinese Medicine
IEC-6 Rat intestinal epithelial cell line-6
PVDF polyvinylidene difluoride
ECL Electro-Chemi-Luminescence

References

1. D. B. Longley, D. P. Harkin and P. G. Johnston, 5-fluorouracil: mechanisms of action and clinical strategies, Nat Rev Cancer, 2003, 3, 330-338.
2. R. A. Ribeiro, C. W. Wanderley, D. V. Wong, J. M. Mota, C. A. Leite, M. H. Souza, F. Q. Cunha and R. C. Lima-Junior, Irinotecan- and 5-fluorouracil-induced intestinal mucositis: insights into pathogenesis and therapeutic perspectives, Cancer Chemother Pharmacol, 2016, 78, 881-893.
3. J. Y. Douillard, D. Cunningham, A. D. Roth, M. Navarro, R. D. James, P. Karasek, P. Jandik, T. Iveson, J. Carmichael, M. Alakl, G. Gruia, L. Awad and P. Rougier, Irinotecan combined with fluorouracil compared with fluorouracil alone as first-line treatment for metastatic colorectal cancer: a multicentre randomised trial, Lancet, 2000, 355, 1041-1047.
4. J. Wang, W. Feng, S. Zhang, L. Chen, Y. Sheng, F. Tang, J. He, X. Xu, H. Ao and C. Peng, Ameliorative effect of Atractylodes macrocephala essential oil combined with Panax ginseng total saponins on 5-fluorouracil induced diarrhea is associated with gut microbial modulation, J Ethnopharmacol, 2019, 238, 111887.
5. R. V. Lalla, M. M. Schubert, R. J. Bensadoun and D. Keefe, Anti-inflammatory agents in the management of alimentary mucositis, Support Care Cancer, 2006, 14, 558-565.
6. D. M. Keefe, Intestinal mucositis: mechanisms and management, Curr Opin Oncol, 2007, 19, 323-327.
7. R. Sharma, P. Tobin and S. J. Clarke, Management of chemotherapy-induced nausea, vomiting, oral mucositis, and diarrhoea, Lancet Oncol, 2005, 6, 93-102.

8. B. Cai, J. Pan, H. Chen, X. Chen, Z. Ye, H. Yuan, H. Sun and P. Wan, Oyster polysaccharides ameliorate intestinal mucositis and improve metabolism in 5-fluorouracil-treated S180 tumour-bearing mice, Carbohydr Polym, 2021, 256, 117545.
9. J. Wu, Y. Gan, M. Li, L. Chen, J. Liang, J. Zhuo, H. Luo, N. Xu, X. Wu, Q. Wu, Z. Lin, Z. Su and Y. Liu, Patchouli alcohol attenuates 5-fluorouracil-induced intestinal mucositis via TLR2/MyD88/NF-kB pathway and regulation of microbiota, Biomed Pharmacother, 2020, 124, 109883.
10. M. B. Zeisel, P. Dhawan and T. F. Baumert, Tight junction proteins in gastrointestinal and liver disease, Gut, 2019, 68, 547-561.
11. H. Chen, F. Zhang, R. Li, Y. Liu, X. Wang, X. Zhang, C. Xu, Y. Li, Y. Guo and Q. Yao, Berberine regulates fecal metabolites to ameliorate 5-fluorouracil induced intestinal mucositis through modulating gut microbiota, Biomed Pharmacother, 2020, 124, 109829.
12. H. L. Li, L. Lu, X. S. Wang, L. Y. Qin, P. Wang, S. P. Qiu, H. Wu, F. Huang, B. B. Zhang, H. L. Shi and X. J. Wu, Alteration of Gut Microbiota and Inflammatory Cytokine/Chemokine Profiles in 5-Fluorouracil Induced Intestinal Mucositis, Front Cell Infect Microbiol, 2017, 7, 455.
13. S. Deng, D. Wu, L. Li, J. Li and Y. Xu, TBHQ attenuates ferroptosis against 5-fluorouracil-induced intestinal epithelial cell injury and intestinal mucositis via activation of Nrf2, Cell Mol Biol Lett, 2021, 26, 48.
14. S. Kato, S. Hayashi, Y. Kitahara, K. Nagasawa, H. Aono, J. Shibata, D. Utsumi, K. Amagase and M. Kadowaki, Saireito (TJ-114), a Japanese traditional herbal medicine, reduces 5-fluorouracil-induced intestinal mucositis in mice by inhibiting cytokine-mediated apoptosis in intestinal crypt cells, PLoS One, 2015, 10, e0116213.
15. A. Atiq, B. Shal, M. Naveed, A. Khan, J. Ali, S. Zeeshan, S. D. Al-Sharari, Y. S. Kim and S. Khan, Diadzein ameliorates 5-fluorouracil-induced intestinal mucositis by suppressing oxidative stress and inflammatory mediators in rodents, Eur J Pharmacol, 2019, 843, 292-306.
16. J. Su, C. Li, X. Yu, G. Yang, J. Deng, Z. Su, H. Zeng, J. Chen, X. Zhang and X. Lai, Protective Effect of Pogostone on 2,4,6-Trinitrobenzenesulfonic Acid-Induced Experimental Colitis via Inhibition of T Helper Cell, Front Pharmacol, 2017, 8, 829.
17. J. Sui, C. Zhang, X. Fang, J. Wang, Y. Li, J. Wang, L. Wang, J. Dong, Z. Zhou, C. Li, J. Chen, T. Ma and D. Chen, Dual role of Ca(2+)-activated Cl(-) channel transmembrane member 16A in lipopolysaccharide-induced intestinal epithelial barrier dysfunction in vitro, Cell Death Dis, 2020, 11, 404.
18. L. Du, J. J. Kim, J. Shen and N. Dai, Crosstalk between Inflammation and ROCK/MLCK Signaling Pathways in Gastrointestinal Disorders with Intestinal Hyperpermeability, Gastroenterol Res Pract, 2016, 2016, 7374197.
19. R. Al-Sadi, S. Guo, D. Ye and T. Y. Ma, TNF-alpha modulation of intestinal epithelial tight junction barrier is regulated by ERK1/2 activation of Elk-1, Am J Pathol, 2013, 183, 1871-1884.
20. C. R. Weber, D. R. Raleigh, L. Su, L. Shen, E. A. Sullivan, Y. Wang and J. R. Turner, Epithelial myosin light chain kinase activation induces mucosal interleukin-13 expression to alter tight junction ion selectivity, J Biol Chem, 2010, 285, 12037-12046.
21. S. Chen, K. Qian, G. Zhang and M. Zhang, Akkermansia muciniphila and its outer membrane protein Amuc_1100 prophylactically attenuate 5-fluorouracil-induced intestinal mucositis, Biochem Biophys Res Commun, 2022, 614, 34-40.
22. T. Zhang, S. H. Lu, Q. Bi, L. Liang, Y. F. Wang, X. X. Yang, W. Gu and J. Yu, Volatile Oil from Amomi Fructus Attenuates 5-Fluorouracil-Induced Intestinal Mucositis, Front Pharmacol, 2017, 8, 786.
23. X. Chu, X. J. Liu, J. M. Qiu, X. L. Zeng, H. R. Bao and J. Shu, Effects of Astragalus and Codonopsis pilosula polysaccharides on alveolar macrophage phagocytosis and inflammation in chronic obstructive pulmonary disease mice exposed to PM2.5, Environ Toxicol Pharmacol, 2016, 48, 76-84.
24. Y. Meng, Y. Xu, C. Chang, Z. Qiu, J. Hu, Y. Wu, B. Zhang and G. Zheng, Extraction, characterization and anti-inflammatory activities of an inulin-type fructan from Codonopsis pilosula, Int J Biol Macromol, 2020, 163, 1677-1686.
25. S. M. Gao, J. S. Liu, M. Wang, T. T. Cao, Y. D. Qi, B. G. Zhang, X. B. Sun, H. T. Liu and P. G. Xiao, Traditional uses, phytochemistry, pharmacology and toxicology of Codonopsis: A review, J Ethnopharmacol, 2018, 219, 50-70.
26. Y. Zou, H. Yan, C. Li, F. Wen, X. Jize, C. Zhang, S. Liu, Y. Zhao, Y. Fu, L. Li, F. Liu, J. Chen, R. Li, X. Chen and M. Tian, A Pectic Polysaccharide from Codonopsis pilosula Alleviates Inflammatory Response and

Oxidative Stress of Aging Mice via Modulating Intestinal Microbiota-Related Gut–Liver Axis, Antioxidants, 2023, 12.
27. J. Li, T. Wang, Z. Zhu, F. Yang, L. Cao and J. Gao, Structure Features and Anti-Gastric Ulcer Effects of Inulin-Type Fructan CP-A from the Roots of Codonopsis pilosula (Franch.) Nannf, Molecules, 2017, 22.
28. G. Pepe, S. F. Rapa, E. Salviati, A. Bertamino, G. Auriemma, S. Cascioferro, G. Autore, A. Quaroni, P. Campiglia and S. Marzocco, Bioactive Polyphenols from Pomegranate Juice Reduce 5-Fluorouracil-Induced Intestinal Mucositis in Intestinal Epithelial Cells, Antioxidants (Basel), 2020, 9.
29. J. H. Liu, C. H. Hsieh, C. Y. Liu, C. W. Chang, Y. J. Chen and T. H. Tsai, Anti-inflammatory effects of Radix Aucklandiae herbal preparation ameliorate intestinal mucositis induced by 5-fluorouracil in mice, J Ethnopharmacol, 2021, 271, 113912.
30. D. Korenaga, M. Honda, M. Yasuda, S. Inutsuka, T. Nozoe and H. Tashiro, Increased intestinal permeability correlates with gastrointestinal toxicity among formulations of the fluorouracil analogue tegafur in rats, Eur Surg Res, 2002, 34, 351-356.
31. C. Tefas, L. Ciobanu, C. Berce, A. Mester, S. Onica, C. Toma, M. Tantau and M. Taulescu, Beneficial effect of oral administration of zinc sulfate on 5-fluorouracil-induced gastrointestinal mucositis in rats, Eur Rev Med Pharmacol Sci, 2020, 24, 11365-11373.
32. X. Y. Wang, B. Zhang, Y. Lu, L. Xu, Y. J. Wang, B. Y. Cai and Q. H. Yao, RNA-seq and In Vitro Experiments Reveal the Protective Effect of Curcumin against 5-Fluorouracil-Induced Intestinal Mucositis via IL-6/STAT3 Signaling Pathway, Journal of immunology research, 2021, 2021, 8286189.
33. D. C. Xiang, J. Y. Yang, Y. J. Xu, S. Zhang, M. Li, C. Zhu, C. L. Zhang and D. Liu, Protective effect of Andrographolide on 5-Fu induced intestinal mucositis by regulating p38 MAPK signaling pathway, Life Sci, 2020, 252, 117612.
34. X. Li, Q. Li, B. Xiong, H. Chen, X. Wang and D. Zhang, Discoidin domain receptor 1(DDR1) promote intestinal barrier disruption in Ulcerative Colitis through tight junction proteins degradation and epithelium apoptosis, Pharmacol Res, 2022, 183, 106368.
35. H. T. Idriss and J. H. Naismith, TNF? and the TNF receptor superfamily: Structure-function relationship(s), Microscopy Research and Technique, 2000, 50, 184-195.
36. S. Huang, Y. Fu, B. Xu, C. Liu, Q. Wang, S. Luo, F. Nong, X. Wang, S. Huang, J. Chen, L. Zhou and X. Luo, Wogonoside alleviates colitis by improving intestinal epithelial barrier function via the MLCK/pMLC2 pathway, Phytomedicine, 2020, 68, 153179.
37. J. Wu, Y. Gan, H. Luo, N. Xu, L. Chen, M. Li, F. Guan, Z. Su, Z. Lin, J. Xie and Y. Liu, beta-Patchoulene Ameliorates Water Transport and the Mucus Barrier in 5-Fluorouracil-Induced Intestinal Mucositis Rats via the cAMP/PKA/CREB Signaling Pathway, Front Pharmacol, 2021, 12, 689491.
38. J. M. Cavaillon, Exotoxins and endotoxins: Inducers of inflammatory cytokines, Toxicon, 2018, 149, 45-53.
39. P. C. Heinrich, I. Behrmann, S. Haan, H. M. Hermanns, G. Muller-Newen and F. Schaper, Principles of interleukin (IL)-6-type cytokine signalling and its regulation, Biochem J, 2003, 374, 1-20.
40. N. Nishimoto and T. Kishimoto, Inhibition of IL-6 for the treatment of inflammatory diseases, Curr Opin Pharmacol, 2004, 4, 386-391.
41. T. Kucharzik, N. Lugering, H. G. Pauels, W. Domschke and R. Stoll, IL-4, IL-10 and IL-13 down-regulate monocyte-chemoattracting protein-1 (MCP-1) production in activated intestinal epithelial cells, Clin Exp Immunol, 1998, 111, 152-157.
42. X. Liu, J. Xu, Q. Mei, L. Han and J. Huang, Myosin Light Chain Kinase Inhibitor Inhibits Dextran Sulfate Sodium-Induced Colitis in Mice, Digestive Diseases and Sciences, 2012, 58, 107-114.
43. Y. Y. Shao, Y. N. Zhao, Y. F. Sun, Y. Guo, X. Zhang, Z. P. Chang, R. G. Hou and J. Gao, Investigation of the internalization and transport mechanism of Codonopsis Radix polysaccharide both in mice and Caco-2 cells, Int J Biol Macromol, 2022, 215, 23-35.
44. J.-h. Chen, C.-l. Zhao, Y.-s. Li, Y.-b. Yang, J.-g. Luo, C. Zhang and L. Wang, Moutai Distiller's grains Polyphenol extracts and rutin alleviate DSS-induced colitis in mice: Modulation of gut microbiota and intestinal barrier function （R2）, Heliyon, 2023, 9.
45. A. Adak and M. R. Khan, An insight into gut microbiota and its functionalities, Cell Mol Life Sci, 2019, 76, 473-493.
46. C. Kong, R. Gao, X. Yan, L. Huang, J. He, H. Li, J. You and H. Qin, Alterations in intestinal microbiota of colorectal cancer patients receiving radical surgery combined with adjuvant CapeOx therapy, Sci China Life Sci, 2019, 62, 1178-1193.

 doi:10.20944/preprints202312.1959.v1

47. E. Kim, D. B. Kim and J. Y. Park, Changes of Mouse Gut Microbiota Diversity and Composition by Modulating Dietary Protein and Carbohydrate Contents: A Pilot Study, Prev Nutr Food Sci, 2016, 21, 57-61.
48. M. Qasim, M. Wrage, B. Nuse and J. Mattner, Shigella Outer Membrane Vesicles as Promising Targets for Vaccination, Int J Mol Sci, 2022, 23.